Improving the Convergence of Shot-Profile Migration by Plane Wave Synthesis

Chad M. Hogan*
University of Calgary, Calgary, AB, Canada
cmhogan@ucalgary.ca

and

Gary F. Margrave
University of Calgary, Calgary, AB, Canada

Summary

Prestack depth migration may be accelerated by the synthesis of carefully-selected plane-wave virtual sources, and deliberate stacking of input shot records. Plane-wave migration drastically reduces the amount of computation required to generate an interpretable seismic image. Here we show quantitative measurements of the rate of convergence of plane-wave images and compare to traditional shot-profile migration.

Introduction

Prestack depth migration is expensive for complex regions with strong lateral velocity variations. In these regions, it is desirable to use a wave-equation migration algorithm such as FOCI (Margrave et al., 2006). Plane-wave migration was developed in part to preserve the fidelity benefits of prestack wave equation techniques while adding the benefits of poststack processing economy (see e.g. Rietveld et al., 1992; Whitmore, 1995; Mosher and Foster, 1998; Duquet et al., 2001; Liu et al., 2002, 2006; Grion and Jakubowicz, 2006). A plane wave is synthesized by the superposition of numerous point sources. This is accomplished by stacking common shot gathers that are time-delayed by a linear function of the shot location. This stack is imaged using a similarly constructed plane wave source model. A zero time-delay corresponds to a horizontal plane wave (i.e. with 0° orientation). Shot delays are a linear function of source position. If the slope of this function is positive, this corresponds to “positive orientation” of the plane wave.

In contrast to usual shot-profile migration, plane-wave migration has the benefit that a useful image can be developed from relatively few individual plane waves. For flat homogeneous layers and a survey with numerous shots and receivers, it is conceivable that only the 0° plane wave could be required to generate a usable image. This is roughly equivalent in cost to a poststack migration. Plane-wave migration has the added benefit that more plane waves with varying orientation may be added to selectively improve the image. This allows fine control of the overall cost of imaging, and allows individuals to choose precisely where they would like to spend their time in imaging.

Theory

The theory of plain-wave migration is explained by several authors. Here we select important concepts as described by Liu et al (2006). A similar treatment may be found in Romero et al. (2000).

Consider a source wavefield of a shot $S_j(\omega,x,z)$, where ω is temporal frequency, x and z are lateral and vertical spatial coordinates, and index $j=1,2,\text{K},N$ where N is the total number of shots. A composite wavefield $\bar{S}(\omega,x,z)$ is expressed as

$$\bar{S}(\omega,x,z)=\sum_{j=1}^{N}a_j(\omega)S_j(\omega,x,z), \tag{1}$$

where the $a_j(\omega)$ are N functions that serve to time-delay shots as required. The composite receiver wavefield $\bar{R}(\omega,x,z)$ is similar, and $R_j(\omega,x,z)$ is the backwards-extrapolated receiver wavefield that corresponds to $S_j(\omega,x,z)$. To compose a 2D plane-wave section simulating a line-source wavefield with ray parameter p,

$$a_j(\omega)=f(\omega)e^{i\omega p(x_j-x_0)}, \tag{2}$$

where $f(\omega)$ is a real function and x_0 is the plane wave origin at the surface.

For wavefield extrapolation operators, Liu et al. (2006) define $\mathbf{L}$ and its conjugate operator $\mathbf{L}^*$ such that

$$S(\omega,x,z)=\mathbf{L}^*[S(\omega,x,z-\Delta z)], \tag{3}$$

$$R(\omega,x,z)=\mathbf{L}[R(\omega,x,z-\Delta z)]. \tag{4}$$

Application of $\mathbf{L}$ to $\bar{S}$ and $\bar{R}$ gives

$$\bar{S}(\omega,x,z)=\mathbf{L}^*[\bar{S}(\omega,x,z-\Delta z)], \tag{5}$$

$$\bar{R}(\omega,x,z)=\mathbf{L}[\bar{R}(\omega,x,z-\Delta z)]. \tag{6}$$

With the application of a crosscorrelation imaging condition, this can be shown to yield an image $I(x,z)$,

$$I(x,z)=\sum_{j=1}^{N}\sum_{\omega}\left|a_j(\omega)\right|^2 S_j^*(\omega,x,z)R_j(\omega,x,z)+\sum_{j\neq k}^{N}\sum_{\omega}a_j^*(\omega)a_k(\omega)S_j^*(\omega,x,z)R_k(\omega,x,z). \tag{7}$$

Liu et al. (2006) describe each term in equation (7). The first is the stack of images for each individual shot, which is the expected output from a shot-profile migration. The second term is described as the results of the crosscorrelation of source wavefields with the receiver wavefields from different shots – "cross terms". This results in an imaging artifact that may be addressed by phase encoding techniques (e.g. Romero et al., 2000).

2D Source Plane-Wave Migration

Using these results, Liu et al. (2006) show that the final image $I(x,z)$ is

$$I(x,z)=\sum_{j=1}^{N}\sum_{k=1}^{N}\sum_{\omega}f^2(\omega)S_k^*(\omega,x,z)R_j(\omega,x,z)\sum_{l=-N_p}^{N_p}e^{i\omega l\Delta p(x_j-x_k)}, \tag{8}$$

where the final sum in equation (8) approximates a delta function in the limit as the number of plane waves $N_p\to\infty$. So, given "enough" plane waves, the cross terms are suppressed. But how many plane waves are "enough"?

Residual Measurement

We propose a simple measure of the convergence of plane-wave imaging. The goal is to quantify the improvement of the image quality with the successive addition of plane waves to the final image. The "residual" is defined in terms of two such images, $I_A(x,z)$ and $I_B(x,z)$. The indices A,B may refer to any pair of images. For example, $I_A(x,z)$ may refer to an image generated by the stacking of 11 distinct plane-wave images, while $I_B(x,z)$ may be the image generated by the stacking of 13 distinct plane-wave images[1]. The two images are spatially localized by a window $\Omega(x,z)$ with values of one inside the region of interest, zero when well outside, and a smooth transition between. The residual $\mathbf{R}(x,z)$, based on the ℓ^2 norm of the difference in the images, is

$$\mathbf{R}(x,z)=\frac{\sqrt{\sum_{x,z}\Omega(x,z)\left(I_A(x,z)-I_B(x,z)\right)^2}}{\sqrt{\sum_{x,z}\Omega(x,z)\left(I_A(x,z)\right)^2}}. \tag{9}$$

Testing and Conclusions

We tested this residual on images of the Marmousi model generated using a number of equally-spaced shot records as usual, and the same number of plane-waves distributed symmetrically about 0°. In Figure 1, the 41-record image may be seen. Neglecting the slant-stacking and source-synthesis steps (which are trivial), the plane-wave and shot-profile image codes run in approximately the same amount of time. This figure demonstrates qualitatively that the plane-wave image is quite respectable compared to the shot-profile image, even at only 41 plane waves. In Figure 2, the 81-record image is shown. The difference is somewhat less dramatic. This effect is clearly quantified by the calculation of residuals. In Figure 3, residuals are shown for successive additions of number of migrations (A and B may correspond to 11 and 13 plane waves or shot records, for example). This is the "instantaneous residual". These residuals demonstrate that the plane-wave migration converges to its final form faster than the shot-profile image for both a shallow region and for the reservoir target, with windows Ω chosen to isolate the circled regions in the right hand side of Figure 1.

Although the instantaneous residual shows that the plane-wave image converges to its final form faster than the shot-profile converges to its final form, the real test is a comparison of the convergences to the final shot-profile image – the image typically accepted as "best". On the right hand side of Figure 3, these "final residuals" are displayed. Here it can be seen that plane-wave

[1] In our implementation, the first image generated uses the horizontal plane wave, and plane waves are added symmetrically, two at a time for each successive image. Thus 13 naturally follows 11.

migration handily beats shot-profile migration at its own game: the final residuals for the plane-wave images decrease faster than those of the shot-profile migration. For example, at about 20 migrations (i.e. 20 plane waves), the plane-wave image has approximately half the final residual of the shot-profile image, and the shot-profile image does not reach this final residual until nearly 50 migrations (i.e. 50 shot records).

Acknowledgements

We thank the CREWES sponsors, POTSI sponsors, NSERC, and the SEG for support in this research. We are also grateful for stimulating discussions with Michael Lamoureux.

References

Duquet, B., Laily, P., and Ehinger, A., 2001: 3D plane wave migration of streamer data: 71st Meeting, Society of Exploration Geophysicists, Expanded Abstracts.

Grion, S., and Jakubowicz, H., 2006, On the influence of Offset in Plane-Wave Migration: 76th Meeting, Society of Exploration Geophysicists, Expanded Abstracts.

Liu, F., Hanson, D., Whitmore, N., Day, R., and Stolt, R., 2006: Toward a unified analysis for source plane-wave migration: Geophysics, **71**, No. 4, S129-S139.

Liu, F., Stolt, R., Hanson, D., and Day, R., 2002: Plane wave source composition: An accurate phase encoding scheme for prestack migration: 72nd Meeting, Society of Exploration Geophysicists, Expanded Abstracts.

Margrave, G., Geiger, H., Al-Saleh, S., and Lamoureux, M., 2006: Improving explicit depth migration with a stabilizing Weiner filter and spatial resampling: Geophysics, **71**, No. 3, S111-S120.

Mosher, C., and Foster, D., 1998: Offset plane wave propagation in laterally varying media: *in* Mathematical Methods in Geophysical Imaging V: Proceedings of SPIE 3453, 36—46.

Rietveld, W., Berkhout, A., and Wapenaar, C., 1992: Optimum seismic illumination of hydrocarbon reservoirs: Geophysics, **57**, 1334—1345.

Romero, L., Ghiglia, D., Ober, C., and Morton, S., 2000: Phase encoding of shot records in prestack migration: Geophysics, **65**, 426—436.

Stork, C., and Kapoor, J., 2004: How many P values do you want to migrate for delayed-shot wave equation migration?: 74th Meeting, Society of Exploration Geophysicists, Expanded Abstracts.

Whitmore, N., 1995: An imaging hierarchy for common angle plane wave seismograms: Ph.D. thesis, University of Tulsa.

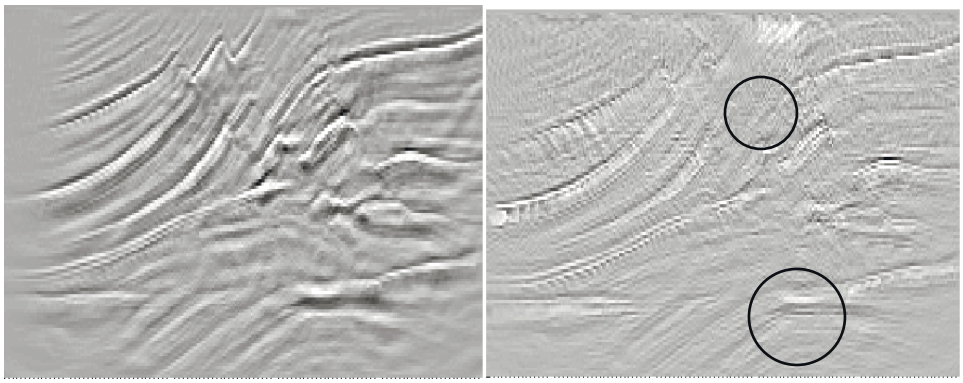

Figure 1. Marmousi image, 41 plane waves (left); 41 shot records (right). Shallow region circled at top, reservoir region circled below.

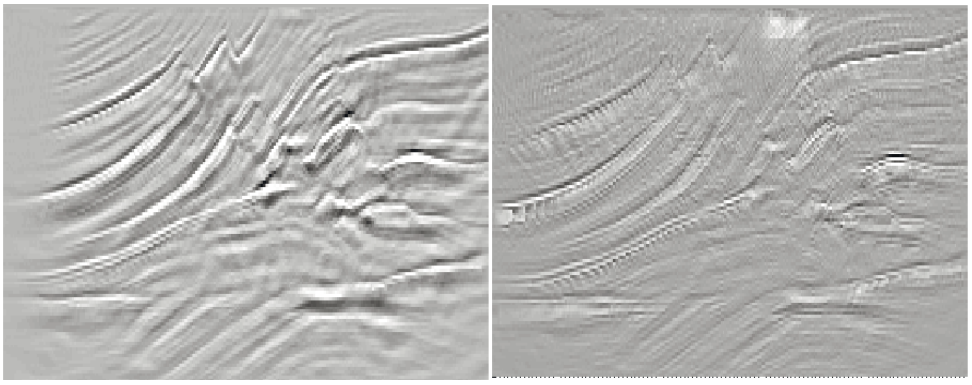

Figure 2. Marmousi image, 81 plane waves (left); 81 shot records (right).

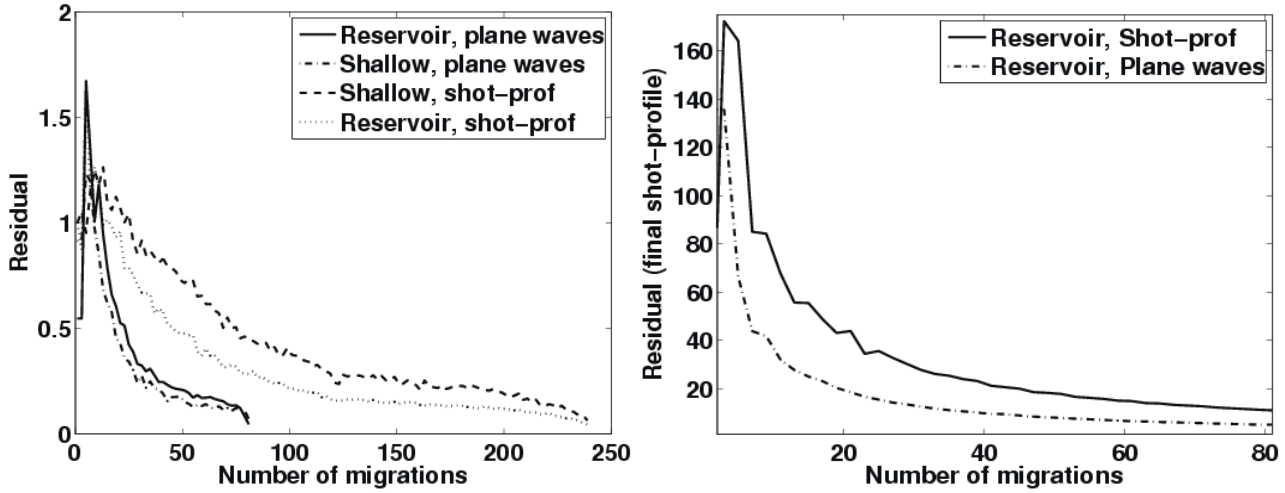

Figure 3. Residuals of plane-wave vs. shot profile. On the left is instantaneous residual. On the right is final residual, i.e. between the N migrations and the final shot-profile image.